CHAPTER 72

VERIFICATION OF A ONE-DIMENSIONAL SURFBEAT MODEL AGAINST LABORATORY DATA

J.A. Roelvink, H.A.H. Petit and J.K. Kostense

DELFT HYDRAULICS, P.O. Box 152, 8300 AD Emmeloord

ABSTRACT

A mathematical model is presented which describes cross-shore low-frequency motions generated by shoaling and breaking of wave-groups on a beach. The numerical scheme is tested against known analytical solutions for standing waves on a plane beach. Model results are compared with laboratory experiments (Kostense, 1984) which refer to bichromatic carrier waves incident on a plane beach. It is shown that, apart from a good representation of the trends found in the experimental study, for realistic values of the breaking and friction coefficients the computational results also quantitatively agree surprisingly well with the experiments.

INTRODUCTION

Low-frequency motions on the time-scale of wave groups can have significant effects on cross-shore morphology, both in the inner nearshore region, where sometimes they even dominate over motions at wind-wave frequencies, and elsewhere in the nearshore region, through their interaction with the wave groups. Their effect on cross-shore morphology has been shown to be of the same order of magnitude as other mechanisms, such as return flow and wave asymmetry (Roelvink and Stive, 1989).

Several aspects of long-wave generation inside and outside the surf zone have been addressed in literature (e.g. Longuet-Higgins and Stewart, 1962; Symonds et al, 1982; Abdelrahman and Thornton, 1987; Schaeffer and Jonsson, 1990; List, 1992). The models presented in these references are strongly schematized in either the hydrodynamic equations or the bottom geometry and are not meant to be predictive models for arbitrary waves on an arbitrary profile. Some first attempts towards this were presented in Roelvink (1991), Symonds and Black (1991) and Sato (1991).

The purpose of the model presented here is to predict the cross-shore structure of the incident wave groups, the long waves generated inside and outside the surfzone, and their combined effect on sediment transport, for random waves incident perpendicular to a uniform beach of arbitrary profile. The model is

time-dependent on the time-scale of wave groups; the basic formulations have been described in Roelvink (1991).

In the paper we will discuss the model formulations; the numerical scheme will be outlined and tested against analytical solutions of parts of the problem. The model is then compared with experiments with bichromatic waves on a plane beach and the sensitivity of the model for the dissipation coefficients is investigated.

MODEL FORMULATIONS

The model solves simultaneously a set of three short-wave averaged balance equations, viz. for momentum, continuity and wave energy. Closure relations which relate i.e. radiation stress to wave energy are derived from linear theory. Wave breaking is incorporated by means of an empirical formulation, which relates the dissipation rate to the local wave energy and the water depth.

The balance equations are: the momentum equation for the long waves,

$$\frac{\partial}{\partial t} Q_t + \frac{\partial}{\partial x} \left[\frac{\left(Q_t^2 - Q_w^2\right)}{h} + \frac{S_{xx}}{\rho} + \frac{1}{2}gh^2 \right] = gh \frac{\partial d}{\partial x} + \tau_b \tag{1}$$

the continuity equation for the long waves,

$$\frac{\partial}{\partial t} h + \frac{\partial}{\partial x} Q_t = 0 \tag{2}$$

and the wave action equation, reduced to a wave energy balance equation:

$$\frac{\partial}{\partial t} E + \frac{\partial}{\partial x} EC_g = -D \tag{3}$$

Here, h is the water depth, Q_t is the total flux, Q_w is the wave-induced flux, S_{xx} is the radiation stress, ρ is the density of the water, g is the acceleration of gravity, d is the still water depth, τ_b is the bottom shear stress, E is the short wave energy and C_g is the group velocity of the short waves.

Additional equations are required to close the system of equations; very common ones are used here:

$$\tau_b = \frac{1}{2}\rho f_w \left| \frac{Q_t}{h} \right| \frac{Q_t}{h} \tag{4}$$

where f_w is a friction coefficient;

$$S_{xx} = \left[2\frac{C_g}{C} - \frac{1}{2} \right] E \tag{5}$$

$$Q_w = \frac{E}{\rho C} \tag{6}$$

$$C = \frac{\omega}{k} \tag{7}$$

$$C_g = \frac{\partial \omega}{\partial k} = \frac{g}{2\omega} \left(\tanh(kh) + kh \left[1 - \tanh^2(kh) \right] \right) \tag{8}$$

Here, ω is a representative angular frequency of the short waves and k is a representative wave number.

The short wave energy dissipation is modelled according to Roelvink (1992) as:

$$D = 2\alpha f E \left[1 - \exp \left(- \left[\frac{\sqrt{8E/\rho g}}{\gamma h} \right]^n \right) \right] \tag{9}$$

where f is a representative short wave frequency and α, γ and n are coefficients, with optimum values for random waves of 1.0, 0.55 and 10, respectively.

With the help of these additional equations, equations (1) through (3) are solved simultaneously for a given profile and boundary conditions for E, Q_t and h at the seaward boundary.

NUMERICAL SCHEME

The differential equations are solved by a finite difference, second-order Richtmeyer scheme on a nonequidistant moving grid of which the landward boundary moves up and down with the waterline. This is achieved by applying a transformation to the equations as described below.

The set of equations we want to transform can in Cartesian coordinates be described as:

$$\frac{\partial v}{\partial t} + \frac{\partial f(v)}{\partial x} = o(v) \frac{\partial p}{\partial x} + q(v) \tag{10}$$

where the functions f and q need not be linear in their arguments.
We now use a transformation to general time dependent coordinates of the following form:

$$\tau = t \tag{11}$$

$$\xi = \frac{\displaystyle\int_0^x W(\zeta) d\zeta}{\displaystyle\int_0^{x_r(t)} W(\zeta) d\zeta} \tag{12}$$

This transformation transforms the interval in the x-domain: $[0, X_r(t)]$ which depends on the time coordinate t, to the fixed interval $[0,1]$ in the ξ domain. The transformation to the τ domain is trivial.

In order that the inverse transformation functions $x(\tau, \xi)$ and $t(\tau)$ exist the function W has to be chosen such that it does not change sign in the interval $[0, X_r(t)]$.

The function $X_r(t)$ is the solution of an ordinary differential equation:

$$\frac{dX_r(t)}{dt} = S(v(t, X_r(t)) = u(t, X_r(t)) \tag{13}$$

In the new coordinate system the set of differential equations becomes:

$$\frac{\partial}{\partial \tau}\left(T_1(\tau, \xi) \, \hat{v}(\tau, \xi)\right) + \frac{\partial}{\partial \xi}\left(T_2(\tau, \xi) \, \hat{v}(\tau, \xi) + f(v(\tau, \xi))\right) = T_1\left(\tau, \xi\right)\left(o(\hat{v}(\tau, \xi)) \, \hat{p}_x(\tau, \xi) + q(\hat{v}(\tau, \xi))\right) \tag{14}$$

$$\frac{dX_r(\tau)}{d\tau} = \hat{u}(\tau, 1) \tag{15}$$

where,

$$T_1(\tau, \xi) = \frac{\displaystyle\int_0^{X_r(\tau)} W(\varsigma)\,d\varsigma}{W(x(\tau, \varsigma))}, \qquad T_2(\tau, \xi) = -\frac{\xi \, W(X_r(\tau))}{W(x(\tau, \xi))} \, \frac{dX_r(\tau)}{d\tau}$$

$$\hat{v}(\tau, \xi) = v(\tau, x(\tau, \xi)) \text{ and } \hat{p}_x(\tau, \xi) = \frac{dp}{dx}(x(\tau, \xi)).$$

In the appendix a derivation of equation (14) is given.
Equation (14) can be written as:

$$\frac{\partial V}{\partial \tau} + \frac{\partial F(V, \tau, \xi)}{\partial \xi} = R(V, \tau, \xi), \tag{16}$$

so it has exactly the same structure as Eq.(10).

The discretization used to solve the set of differential equations (14) in the (τ, ξ) domain is done on an equidistant grid:

$$\xi_i = \frac{i}{N} \text{ for } i = 0(1)N.$$

The time steps are constant as well: $\tau_j = j\Delta\tau$ and therefore $t_j = j\Delta\tau$.

In the physical domain (t, x) this introduces a non-equidistant grid with grid points x_i^j which satisfy the equation:

$$\xi_i = \frac{i}{N} = \frac{\displaystyle\int_0^{x_i^j} W(\varsigma)\,d\varsigma}{\displaystyle\int_0^{X_r(\tau_j)} W(\varsigma)\,d\varsigma} \qquad \text{for } i = 0(1)N \tag{17}$$

The weight function W can be chosen in such a way that near to regions where the physics becomes more interesting a grid refinement can be realized.

The scheme we use is Richtmeyer's predictor corrector scheme; the discretization of Eq.(16) now becomes:

Predictor:

$$V_{i+1/2}^{j+1/2} = \frac{1}{2}(V_{i+1}^j + V_i^j) - \frac{\Delta\tau}{2\Delta\xi}(F_{i+1}^j - F_i^j) + \frac{\Delta\tau}{4}(R_{i+1}^j + R_i^j) \qquad (18)$$

where $F_{i+1}^j = F(V_{i+1}^j, \tau_j, \xi_{i+1})$, $R_{i+1}^j = R(V_{i+1}^j, \tau_j, \xi_{i+1})$,

$F_{i+1/2}^{j+1/2} = F(V_{i+1/2}^{j+1/2}, \tau_{j+1/2}, \xi_{i+1/2})$ and $R_{i+1/2}^{j+1/2} = R(V_{i+1/2}^{j+1/2}, \tau_{j+1/2}, \xi_{i+1/2})$

$$X_r^{j+1/2} = X_r^j + \frac{\Delta\tau}{48}(34\,\hat{u}(\tau_j, 1) - 14\,\hat{u}(\tau_{j-1}, 1) + 4\,\hat{u}(\tau_{j-2}, 1)) \qquad (19)$$

$x_{i+1/2}^{j+1/2}$ is solved from $\xi_{i+1/2} = \dfrac{i+1/2}{N} = \dfrac{\displaystyle\int_0^{x_{i+1/2}^{j+1/2}} W(\zeta)\,d\zeta}{\displaystyle\int_0^{x_r^{j+1/2}} W(\zeta)\,d\zeta}$ for $i = 0(1)N-1$.

Corrector:

$$V_i^{j+1} = V_i^j - \frac{\Delta\tau}{\Delta\xi}(F_{i+1/2}^{j+1/2} - F_{i-1/2}^{j+1/2}) + \frac{\Delta\tau}{2}(R_{i+1/2}^{j+1/2} + R_{i-1/2}^{j+1/2}) \qquad (20)$$

$$X_r^{j+1} = X_r^j + \frac{\Delta\tau}{12}(23\,\hat{u}(\tau_j, 1) - 16\,\hat{u}(\tau_{j-1}, 1) + 5\,\hat{u}(\tau_{j-2}, 1)) \qquad (21)$$

x_i^{j+1} is solved from: $\xi_i = \dfrac{i}{N} = \dfrac{\displaystyle\int_0^{x_i^{j+1}} W(\zeta)\,d\zeta}{\displaystyle\int_0^{x_r^{j+1}} W(\zeta)\,d\zeta}$,for $i = 0(1)N$.

The schemes that are used to solve Eq.(15) are (19) and (21), these are both third order Adams-Bashforth methods.

The linear stability condition for the Richtmeyer scheme is

$$\frac{\lambda\Delta\tau}{\Delta\xi} \le 1 \qquad (22)$$

where λ is the largest eigenvalue of $\partial F/\partial V$ in absolute sense.

The largest eigenvalue of $\partial f/\partial v$ in equation (10) can be approximated by $u + \sqrt{gh}$. Since T_1 and T_2 are both scalar functions, the largest eigenvalue in the transformed problem (14) becomes:

$$\lambda = \frac{T_2}{T_1} + \frac{\hat{u} + \sqrt{g\hat{h}}}{T_1}$$

Stability condition (22) can now be written as:

$$W(x(\tau,\xi))\,\hat{u}(\tau,\xi) - \xi\,W(X_r(\tau))\,\frac{dX_r}{d\tau} + W(x(\tau,\xi))\,\sqrt{g\hat{h}(\tau,\xi)} \;\leq\; \frac{\Delta\xi}{\Delta\tau}\int\limits_{0}^{X_r(\tau)} W(\zeta)\,d\zeta \tag{23}$$

The condition we use to replace Eq.(23) is:

$$W(x(\tau,\xi))\,\sqrt{g(\hat{h}(0,\xi)+\epsilon)} \;\leq\; \frac{\Delta\xi}{\Delta\tau}\int\limits_{0}^{X_r(\tau)} W(\zeta)\,d\zeta \tag{24}$$

here $\hat{h}(0,\xi)$ is the still water depth and ϵ is a small positive number.
A convenient weight function now becomes:

$$W(x) = \frac{1}{\sqrt{g\,(h(0,x)+\epsilon)}}$$

With this choice the CFL stability condition (23) can now be replaced by:

$$\Delta\tau \leq \Delta\xi \int\limits_{0}^{X_r(\tau)} \frac{1}{\sqrt{g\,(h(0,x)+\epsilon)}}\,dx \tag{25}$$

By replacing $X_r(\tau)$ in Eq.(25) by a lower boundary of $X_r(\tau)$ we found a constant value for $\Delta\tau$.

The scheme is compared with analytical solutions of standing long waves on a plane beach as given by Carrier and Greenspan (1957); an example is given in Figure 1. Very small deviations occur at the shoreline, which disappear with increasing number of grid points.

MODEL RESULTS AND SENSITIVITY ANALYSIS

Model results are compared with laboratory experiments by Kostense (1984), which refer to wave channel tests of bichromatic waves on a plane beach. The experiments were carried out with active wave absorption and second order wave generation, enabling undisturbed, stable and accurate measurements. They cover a range of primary frequencies, group frequencies, amplitudes and modulation rates and are therefore well suited to verify the predictive ability of the model. The primary waves in these tests were made up of two frequencies generated in a water depth of 0.50 m and broke on a plane cemented beach of a 1:20 slope after travelling over a horizontal stretch. In Table 1 below, the ranges of frequency and amplitude of the primary waves are given. In series A, B and E, the effect of varying the difference frequency is studied for fixed primary wave amplitudes; in series C and D the effect of varying the primary wave amplitude is shown for a fixed difference frequency. Series A through D were carried out with weakly modulated waves; series E with strongly modulated primary waves.

For a given set of primary waves, the input boundary conditions for the numerical model are defined by:

$$E = \rho g \left[\frac{1}{2}(\hat{\eta}_1^2 + \hat{\eta}_2^2) + \hat{\eta}_1\hat{\eta}_2\cos(\Delta\omega\ t) \right] \tag{26}$$
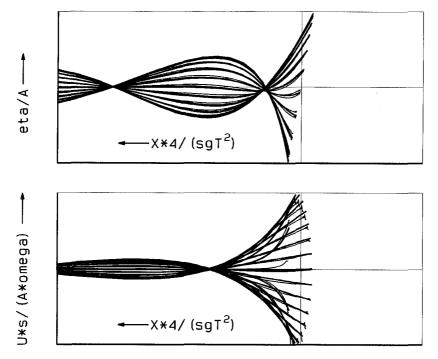
Figure 1.   Comparison of numerical (thin lines) and analytical (thick lines) solution of standing long wave on a plane sloping beach; dimensionless elevation (top) and velocity (bottom).

Series	$\hat{\eta}_1$	$\dfrac{\hat{\eta}_2}{\hat{\eta}_1}$	ω_1	$\Delta\omega$
	(m)	(m)	(rad/s)	(rad/s)
A	0.055	0.2	3.1	0.3-0.9
B	0.055	0.2	4.1	0.3-0.9
C	0.035-0.080	0.2	4.1	0.77
D	0.030-0.055	0.2	3.1	0.61
E	0.035	0.8	4.3	0.3-0.9

Table 1. Ranges of primary wave parameters in Kostense experiment.

The accompanying bound long wave, which is also generated in the experiment, is given by Longuet-Higgins and Stewart (1964):

$$h-\overline{h} = -\frac{1}{\rho}\left[(2\frac{C_g}{C}-0.5) / (gh - C_g^2)\right] \hat{\eta}_1\hat{\eta}_2\cos(\Delta\omega\ t) \qquad (27)$$

$$Q_t = -\frac{C_g}{\rho}\left[(2\frac{C_g}{C}-0.5)/(gh - C_g^2)\right]\hat{\eta}_1\hat{\eta}_2\cos(\Delta\omega\ t) \tag{28}$$

In order to prevent re-reflection of long waves at the seaward boundary, a weakly reflective boundary condition is used as described in Roelvink (1991).

The procedure to hindcast these the experiments is as follows. For a given set of primary waves, the model is run until a periodic solution is reached. The surface elevation time series are then split into three components, viz. the incoming bound wave, the reflected free wave and an incoming free wave. Incoming free waves are negligible since they are not generated and since the weakly reflective boundary condition allows waves reflected from the beach to propagate out of the model. The amplitudes of the incoming bound wave and the reflected free wave are determined by harmonic analysis. Per series A through E, approximately twenty such runs are carried out to cover the range of the free parameter for each series.

The numerical model contains empirical coefficients in the description of the dissipation of short waves by wave breaking, and of the dissipation of long waves by bottom friction. For random waves, a standard set of values for the wave breaking coefficients can be applied, as is shown in Roelvink (1992). A key factor here is the coefficient γ, which is proportional to the average breaking wave height over water depth ratio, and is set at 0.55 for random waves. For bichromatic waves, this ratio should be significantly higher; a reasonable estimate appears to be 0.75. Because of the uncertainty in this value, computations are performed for γ-values of 0.55, 0.75 and 0.90.

Since there is no accurate description of the bottom friction under combined short and long waves, the simplest possible formulation as in eq. (4) is applied. Computations are performed for three values of f_w: 0.00, 0.02 and 0.05. The variations in f_w are applied for a fixed γ-value of 0.75; the variations in γ for a fixed f_w-value of 0.02.

The results for series A through E are shown in Figures 2 through 6, respectively. In all cases, the bound long wave amplitude is predicted accurately; it does not depend on either of the coefficients. The increase in the bound wave amplitude for increasing difference frequency is due to the slight decrease in the mean of the primary frequencies. As expected, the bound wave amplitude increases quadratically with increasing primary wave amplitude.

The amplitudes of the reflected free waves show interesting interference patterns which are represented quite well by the model. Schaffer and Jonsson (1990) already concluded based on a comparison between their model and these data, that frictional effects must be important. Especially for the higher group frequencies this appears to be the case. A reasonable value for the friction factor of 0.02 appears to give acceptable quantitative agreement for all series.
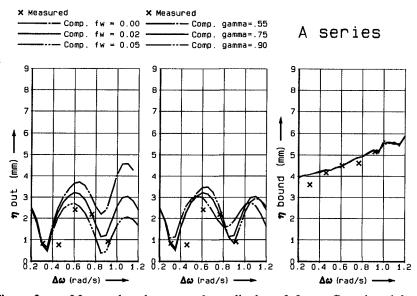
Figure 2.   Measured and computed amplitudes of free reflected and bound long wave elevation against difference frequency $\Delta\omega$; series A.
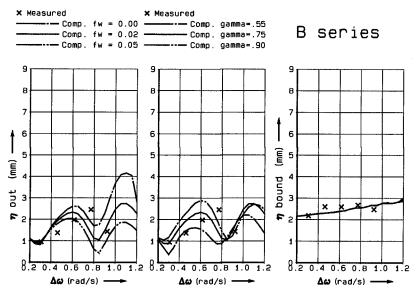

Figure 3.   Measured and computed amplitudes of free reflected and bound long wave elevation against difference frequency $\Delta\omega$; series B.

× Measured   **× Measured**
———·— Comp. fw = 0.00   ———·— Comp. gamma=.55   **C series**
——— Comp. fw = 0.02   ——— Comp. gamma=.75
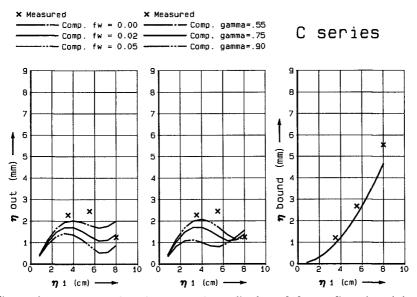———··— Comp. fw = 0.05   ———···— Comp. gamma=.90

Figure 4. Measured and computed amplitudes of free reflected and bound long wave elevation against primary wave amplitude $\hat{\eta}_1$; series C.
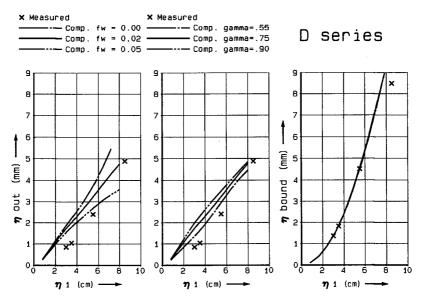
× Measured   **× Measured**
———·— Comp. fw = 0.00   ———·— Comp. gamma=.55   **D series**
——— Comp. fw = 0.02   ——— Comp. gamma=.75
———··— Comp. fw = 0.05   ———···— Comp. gamma=.90

Figure 5. Measured and computed amplitudes of free reflected and bound long wave elevation against primary wave amplitude $\hat{\eta}_1$; series D.

x Measured   **x** Measured
——·—— Comp. fw = 0.00 ——·—— Comp. gamma=.55   E series
———— Comp. fw = 0.02 ———— Comp. gamma=.75
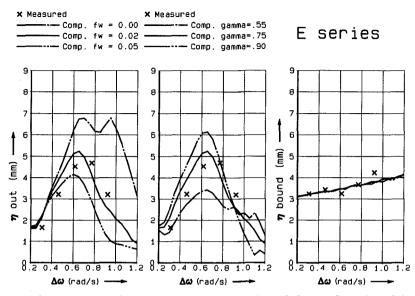——·—— Comp. fw = 0.05 ——··—— Comp. gamma=.90

Figure 6. Measured and computed amplitudes of free reflected and bound long wave elevation against difference frequency $\Delta\omega$; series E.

The model results are not extremely sensitive to variations in the breaker parameter γ. A reasonable value of 0.75 for these bichromatic waves gives acceptable results for all series.

The prediction of the reflected free wave amplitude for highly modulated waves in series E is quite accurate; no previous model results on this case have been presented in literature.

A disadvantage of this numerical model is, that it is not possible to separate different mechanisms of long wave generation, viz. the reflection of bound long waves, the break point mechanism or the shoreline set-up mechanism. Probably all of these mechanisms are important at times; the results indicate that no serious errors in the representation of any mechanism have been made.

CONCLUSION
The numerical model SURFBEAT appears to contain the necessary physics to predict long wave generation in the nearshore zone. Since it can be run with arbitrary boundary conditions over an arbitrary profile, it can be used to model realistic situations where cross-shore processes are dominant.

ACKNOWLEDGEMENT

REFERENCES

Abdelrahman, S.M. and E.B. Thornton (1987)
'Changes in the short wave amplitude and wave number due to the presence of infragravity waves'; Proc., Specialty Conf. Coastal Hydrodynamics, pp. 458-478, ASCE, New York, 1987.

Kostense, J.K. (1984)
'Measurements of surf beat and set-down beneath wave groups'; Proc., 19th Int. Conf. Coastal Eng., Houston.

List, J.H. (1992)
'A model for two-dimensional surfbeat'
J. Geophys. Res., Vol. 97, pp. 5623-5635.

Longuet-Higgins, M.S. and R.W. Stewart (1962)
'Radiation stress and mass transport in gravity waves, with application to "surf beats"'; J. Fluid Mech., 12, pp. 481-504, 1962.

Roelvink, J.A. and M.J.F. Stive (1989)
'Bar generating cross-shore flow mechanisms on a beach'
J. Geophys. Res., Vol. 94, no. C4., pp. 4785-4800, April 15, 1989.

Roelvink, J.A. (1991)
'Modelling of cross-shore flow and morphology'; Proc. ASCE Conf. "Coastal Sediments '91", Seattle, pp. 603-617.

Roelvink, J.A. (1992)
'Dissipation in random wave groups incident on a beach'
to appear in Coastal Engineering.

Sato, S. (1991)
'A numerical model of beach profile change due to random waves' Proc. ASCE Conf. "Coastal Sediments '91", Seattle, pp. 674-687.

Schaffer,H.A. and I.G. Jonsson (1990)
'Theory versus measurements in two-dimensional surf beats'
Proc. 22nd Int. Conf. Coastal Eng., Delft, pp. 1131-1143.

Symonds, G. and K.P. Black (1991)
'Numerical simulation of infragravity response in the nearshore' Proc. 10th Australasion Conf. on Coastal and Ocean Engineering, Auckland, New Zealand, Dec. 1991, pp 339-344.

Symonds, G., D.A. Huntley and A.J. Bowen (1982)
'Long wave generation by a time-varying breakpoint'
J. Geophys. Res., Vol. 87, no C1, pp. 492-498, 1982.

APPENDIX

The transformation equations (11) and (12) are of the form:

$$\tau = t \tag{A1}$$

$$\xi = \xi(t,x) \tag{A2}$$

We can directly see that

$$\frac{\partial \tau}{\partial t} = 1$$

$$\frac{\partial \tau}{\partial x} = 0$$

The property $\dfrac{\partial \tau}{\partial t}\dfrac{\partial \xi}{\partial x} - \dfrac{\partial \tau}{\partial x}\dfrac{\partial \xi}{\partial t} = \dfrac{\partial \xi}{\partial x} \neq 0$ implies that $x(\tau,\xi)$ and $t(\tau,ksi)(\equiv \tau)$ exist.

Obviously the inverse transformation has the property:

$$\frac{\partial t}{\partial \tau} = 1$$

$$\frac{\partial t}{\partial \xi} = 0$$

Since $\dfrac{\partial t}{\partial \xi} = 0$ we find:

$$1 = \frac{\partial \xi}{\partial \xi} = \frac{\partial \xi}{\partial x}\frac{\partial x}{\partial \xi} + \frac{\partial \xi}{\partial t}\frac{\partial t}{\partial \xi} = \frac{\partial \xi}{\partial x}\frac{\partial x}{\partial \xi}, \text{ resulting in:}$$

$$\frac{\partial \xi}{\partial x} = (\frac{\partial x}{\partial \xi})^{-1} \tag{A3}$$

Since $\dfrac{\partial \tau}{\partial t} = 1$ and x and t are independent we have:

$$0 = \frac{\partial x}{\partial t} = \frac{\partial x}{\partial \xi}\frac{\partial \xi}{\partial t} + \frac{\partial x}{\partial \tau}\frac{\partial \tau}{\partial t} = \frac{\partial x}{\partial \xi}\frac{\partial \xi}{\partial t} + \frac{\partial x}{\partial \tau}, \text{ resulting in:}$$

$$\frac{\partial \xi}{\partial t} = -\frac{\partial x}{\partial \tau}(\frac{\partial x}{\partial \xi})^{-1} \tag{A4}$$

The differential equation:

$$\frac{\partial v}{\partial t} + \frac{\partial f}{\partial x} = r,$$

which is one of the components of Eq.(1) to (3), can now directly be written as:

$$\frac{\partial \hat{v}}{\partial \xi}\frac{\partial \xi}{\partial t} + \frac{\partial \hat{v}}{\partial \tau}\frac{\partial \tau}{\partial t} + \frac{\partial \hat{f}}{\partial \xi}\frac{\partial \xi}{\partial x} + \frac{\partial \hat{f}}{\partial \tau}\frac{\partial \tau}{\partial x} = \hat{r},$$

where $\hat{v}(\tau,\xi) = v(\tau,x(\tau,\xi))$ and $\hat{f} = f(\hat{v}(\tau,\xi))$.

With the use of Eqs.(A1),(A2),(A3) and (A4) this becomes:

$$-\frac{\partial x}{\partial \tau}(\frac{\partial x}{\partial \xi})^{-1}\frac{\partial \hat{v}}{\partial \xi}+\frac{\partial \hat{v}}{\partial \tau}+(\frac{\partial x}{\partial \xi})^{-1}\frac{\partial \hat{f}}{\partial \xi}=\hat{r}.$$

Multiplication with $\frac{\partial x}{\partial \xi}$ yields:

$$-\frac{\partial x}{\partial \tau}\frac{\partial \hat{v}}{\partial \xi}+\frac{\partial x}{\partial \xi}\frac{\partial \hat{v}}{\partial \tau}+\frac{\partial \hat{f}}{\partial \xi}=\frac{\partial x}{\partial \xi}\hat{r},$$

which can be written as:

$$\frac{\partial}{\partial \tau}(\frac{\partial x}{\partial \xi}\hat{v})+\frac{\partial}{\partial \xi}(-\frac{\partial x}{\partial \tau}\hat{v}+\hat{f})=\frac{\partial x}{\partial \xi}\hat{r} \tag{A5}$$

With the use of the expressions:

$$\frac{\partial \xi}{\partial t}=-\frac{\int_{0}^{x}W(\varsigma)d\varsigma}{(\int_{X_r(t)}^{}W(\varsigma)d\varsigma)^2}W(X_r(t))\frac{dX_r}{dt}$$

$$\frac{\partial \xi}{\partial x}=\frac{W(x)}{\int_{0}^{X_r(t)}W(\varsigma)d\varsigma}$$

and the relations (A3) and (A4), equation (14) emerges from (A5)